Thin-Layer Electrochemistry of 1,3-Diferrocenyl-2-buten-1-one: Direct Correlation between Driving Force and Liquid/Liquid Interfacial Electron Transfer Rates

Jie Xu,[†] Amir Frcic,[†] Jason A. C. Clyburne,[†] Robert A. Gossage,[‡] and Hua-Zhong Yu*,[†]

Department of Chemistry, Simon Fraser University, Burnaby, British Columbia V5A 1S6, Canada, and Department of Chemistry, Acadia University, Wolfville, Nova Scotia B0P 1X0, Canada

Received: February 27, 2004

The cyclic voltammetric behavior of 1,3-diferrocenyl-2-buten-1-one (abbreviated as **DFcB**), a novel molecule with two electrochemically nonequivalent redox centers, was investigated by the thin-layer method, a simple protocol reported recently for studying electron transfer reactions at liquid/liquid interfaces. The bimolecular rate constants for the two-step electron transfer reactions between **DFcB** in the organic phase and $[Fe(CN)_6]^{4-}$ located in the adjacent aqueous phase were obtained simultaneously at a single interface. The observed clear dependence of the rate constants on the overall driving force (dominated by the apparent formal potentials of the ferrocenyl groups in **DFcB)** is consistent with previous studies and qualitatively in agreement with the conventional Butler−Volmer treatment. The results demonstrate the feasibility of using molecules containing multiple redox centers to study the correlation between the thermodynamic driving force and electron transfer kinetics at liquid/liquid interfaces.

1. Introduction

The interface between two immiscible electrolyte solutions (ITIES) has been proposed as a simple model for understanding membrane chemistry, particularly for examining electron transfer processes occurring in living organisms between redox centers located in media of different polarities.[1−3] In retrospect, the study of charge transfer across ITIES has relied primarily on the development of experimental approaches to construct and polarize the interface.[2,3] An early work by Samec et al. in 1977,[4] which introduced the concept of a four-electrode potentiostat, essentially led the way to the modern studies of both interfacial structures and charge transfer reactions across ITIES. Schiffrin and Girault have contributed significantly to the understanding of electron transfer kinetics at liquid−liquid interfaces based on conventional electrochemical methods.[5] In the 1990s, scanning electrochemical microscopy (SECM) was adapted to the study of charge transfer processes by Bard and others.[6−8] As one of the newest experimental methods, SECM resolves many of the difficulties associated with traditional electrochemical methods including the IR drop, charging current, and distinction between electron transfer and ion transfer processes.[6a] Nevertheless, the limitations of SECM include the construction of the apparatus and the necessity to simulate the kinetic parameters by comparison of experimental and theoretical data.[6−8] Recently, Shi and Anson reported a related but less complex approach by depositing a thin layer of an organic solvent on the electrode surface to examine the electron transfer process between the thin layer and the adjacent aqueous solution.[9] This simple methodology of thin-layer electrochemistry has been readily adopted by other research groups for related studies.[10−12]

What is the correlation between the overall thermodynamic driving force and electron transfer kinetics across an ITIES? Previous investigations have obtained inconclusive answers to this fundamental question.[6−10] The overall driving force is composed of the difference between the formal potentials of the two redox couples in their respective phases and $\Delta_w^o\phi$, the Galvani potential difference at the liquid/liquid interface.[2] The value of $\Delta_w^o\phi$ can be easily changed by adjusting the concentration of the potential-determining ion (e.g., $[ClO_4]^-$, an ion that moves across the liquid/liquid interface); therefore, studies of the driving force dependence of electron transfer kinetics across an ITIES have been largely focused on the modulation of $\Delta_w^o\phi$ at the interface.[6c,7a,8,9c,e] An alternative approach to change the overall driving force is the use of different redox couples either in the aqueous phase[6d,9c] or in the organic phase.[9e] Shi and Anson have recently reported a simultaneous evaluation of electron transfer rate constants of a reactant (e.g., $[Fe(CN)_6]^{3-}$) in aqueous phase with a pair of redox co-reactants (two hydrophobic ferrocene derivatives) at a single interface.[9e] Although this is an elegant experiment that eliminated many uncontrollable factors, its limitations are still obvious: it is not easy to keep the concentrations of the two redox co-reactants in the organic phase identical, and their diffusion coefficients may also differ substantially.

In the present paper, we describe a novel electron transfer system in which 1,3-diferrocenyl-2-buten-1-one (**DFcB**), an α,β-unsaturated ketone with two electrochemically nonequivalent ferrocenyl substituents,[13−16] serves as the redox complex in the organic phase. The remarkable features of the thin-layer method invented by Shi and Anson,[9a] particularly its simplicity of operation and the requirement of very small amounts of reactants, make it suitable for our study. The key advantage of this system is that it permits an examination of the electron transfer kinetics and its effect on the overall driving forces by comparing the rate constants determined for the two redox centers on the same reactant at a single interface (while maintaining the Galvani potential difference $\Delta_w^o\phi$ constant). We focused our research on (a) the thin-layer voltammetric behavior of **DFcB** and its comparison with solution electrochemistry; (b) evaluation of the bimolecular rate constants for electron transfer reactions between **DFcB** in the organic phase

* To whom correspondence should be addressed. Fax: (604) 291-3765. E-mail: hzyu@sfu.ca.
[†] Simon Fraser University.
[‡] Acadia University.

10.1021/jp049104c CCC: $27.50
Published on Web 04/13/2004

and $[Fe(CN)_6]^{4-}$ in the aqueous phase; and (c) comparison of the experimental results obtained with different supporting electrolytes in the aqueous phase (i.e., variation of the formal potential of $[Fe(CN)_6]^{4-}$).

2. Experimental Section

Chemicals. Potassium ferrocyanide(II) hydrate (99.99+%) was obtained from Aldrich; sodium perchlorate (98+%) from Caledon Laboratories Ltd; sodium chloride (99%) from BDH Chemicals Canada Ltd; tetraethylammonium perchlorate (TEAP) from Eastman Kodak Co; and hydrochloric acid (37%) from Fisher Scientific. All above chemicals were used as received.

Nitrobenzene (**NB**) (99.5+%) was obtained from Fluka, purified by washing with dilute acid (0.1 M HCl) and base (0.1 NaOH) solutions, and saturated with deionized water. **DFcB** was synthesized in our laboratory by treating acetylferrocene with $SiCl_4$ in ethanol, and the compound was purified by column chromatography.[16] The identity and purity of **DFcB** were confirmed by ^{1}H NMR spectroscopy, melting point, and X-ray diffraction.[13−16]

Apparatus and Procedures. A conventional glass cell was used for the electrochemical measurements. The working electrode is a cylindrical edge-plane graphite (EPG) rod that was sealed with heat shrink tubing with a 0.42 cm^2 geometric exposure area. It was polished with 600-grit sand paper, then washed and sonicated in deionized water. After the electrode surface was carefully dried with a heat gun, a drop of **NB** (1.0 μL) was gently applied. The solvent spread spontaneously over the hydrophobic surface to form a thin layer (~24 μm thick, as estimated from the volume of the **NB** and the surface area of the electrode). An Ag|AgCl|3 M NaCl and a Pt wire were used as reference and counter electrode, respectively. The working, reference, and counter electrodes were carefully placed in the aqueous phase containing appropriate supporting electrolytes and presaturated with **NB**.[9] Cyclic voltammetry was performed with an Autolab Electrochemical Analyzer (PGSTAT30, Eco Chemie BV, Netherlands) in a Faraday cage. All measurements were repeated at least three times to ensure reproducibility.

3. Results and Discussion

1,3-Diferrocenyl-2-buten-1-one (**DFcB**), the bifunctional redox molecule used for our interfacial electron transfer studies, is the self-condensation product of acetylferrocene.[13−15] It is readily prepared by the treatment of commercially available acetylferrocene with $SiCl_4$ in anhydrous ethanol.[16]

The thin-layer protocol invented by Shi and Anson,[9a] i.e., the method of coating an electrode with a thin layer of organic solution, has been adopted successfully to the examination of the electrochemical behavior of hydrophobic redox complexes.[12,17] Figure 1A shows the cyclic voltammogram of 0.11 mM **DFcB** in the **NB** layer coated on a graphite electrode; the aqueous phase contains only supporting electrolytes (0.1 M NaCl and 0.1 M $NaClO_4$). Little change is observed on repeated potential scans, indicating that the partitioning of **DFcB** into the aqueous phase is negligible.[10] The appearance of two pairs of well-defined, nearly symmetrical redox peaks demonstrates that **DFcB** undergoes two consecutive oxidation/reduction processes under potential control (Scheme 1). This is consistent with the voltammetric behavior of **DFcB** in acetonitrile solution, for which two pairs of diffusing oxidation/reduction peaks were evident.[15] The observed electrochemical inequality shows strong intramolecular electronic communication between the two ferrocenyl moieties.[18] When one of them is oxidized, the strongly electron-withdrawing monocation $FcCOCH{=}C(CH_3)$-

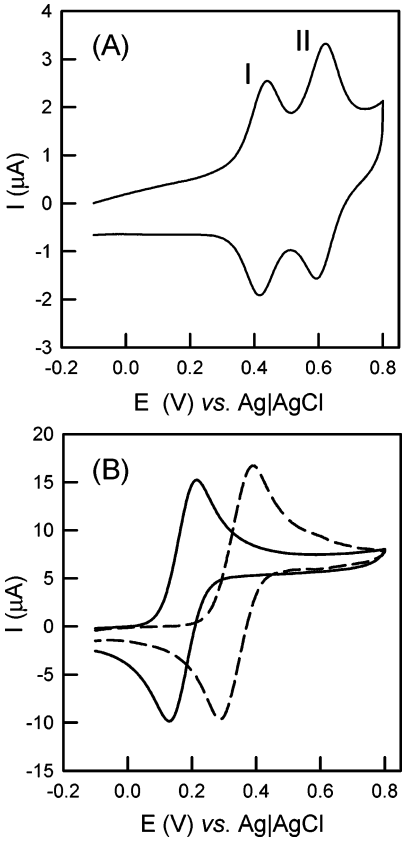

Figure 1. (A) Cyclic voltammogram recorded at a graphite electrode covered with 1.0 μL of nitrobenzene (**NB**) containing 0.11 mM **DFcB**. The supporting electrolyte was 0.1 M tetraethylammonium perchlorate (TEAP) in the **NB** phase; 0.1 M NaCl + 0.1 M $NaClO_4$ in the aqueous phase. The scan rate was 10 mV/s. (B) Cyclic voltammograms recorded at a bare graphite electrode in 1.0 mM $[Fe(CN)_6]^{4-}$. Supporting electrolytes: 0.1 M NaCl + 0.1 M $NaClO_4$ (solid line), 0.1 M HCl + 0.1 M $NaClO_4$ (dashed line). The scan rate was 5 mV/s.

SCHEME 1

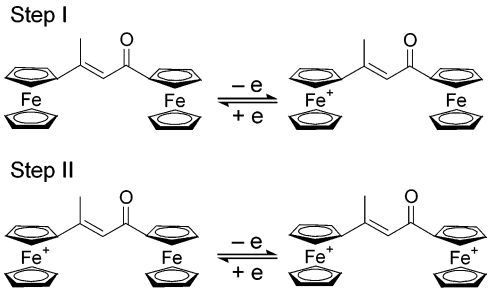

Fc^+ is formed, which leads to the oxidation of the second ferrocenyl group to the dication, $Fc^+COCH{=}C(CH_3)Fc^+$, at a more positive potential. The apparent formal potentials of the two ferrocenyl groups, as calculated from $E^{\circ\prime}_{NB} = (1/2)(E_{pa} + E_{pc})$, are 405 and 580 mV, respectively, with respect to an Ag|AgCl|3 M NaCl reference electrode in the aqueous phase. The difference between the two (ΔE = 175 mV) is close to that reported for the solution electrochemistry of **DFcB** (ΔE = 348−183 = 165 mV, i.e., 183 and 348 mV vs $Ag|Ag^+$ for the two ferrocenyl groups).[15] Such a large formal potential difference is of great interest for the study of electron transfer kinetics across an ITIES, as it provides a unique opportunity for easy modulation of the overall driving force for interfacial electron transfer reactions (see discussion below).

As mentioned above, the thermodynamic driving force is composed of the difference between the formal potentials of

TABLE 1: Bimolecular Rate Constants for Cross-Phase Electron Transfer Reactions between DFcB and $[Fe(CN)_6]^{4-}$ in Adjoining NB/H_2O Phases

	supporting electrolyte in H_2O	$E^{\circ\prime}_{H_2O}$ (mV)[a]	$E^{\circ\prime}_{NB}$ (mV)[b]	overall driving force (mV)[c]	K_{eq}[d]	k_{et} (cm s^{-1} M^{-1})[e]
I	0.1 M $NaClO_4$ + 0.1 M NaCl	200	405	205	2.9×10^3	2.8
II	0.1 M $NaClO_4$ + 0.1 M NaCl	200	583	383	3.0×10^6	3.2
I	0.1 M $NaClO_4$ + 0.1 M HCl	348	406	58	9.6	1.5
II	0.1 M $NaClO_4$ + 0.1 M HCl	348	579	231	8.1×10^3	6.4

[a] Formal potential of the $[Fe(CN)_6]^{3-/4-}$ couple in the aqueous phase. [b] Apparent formal potential of the $\mathbf{DFcB}^{2+/+}$ (II) and the $\mathbf{DFcB}^{+/0}$ (I) couple in the NB thin layer. [c] Calculated from $E^{\circ\prime}_{NB} - E^{\circ\prime}_{H_2O}$. [d] Equilibrium constant of the cross-phase reaction: $\ln K_{eq} = F[E^{\circ\prime}_{NB} - E^{\circ\prime}_{H_2O}]/RT$. [e] Calculated from eqs 1−3. The values of k_{et} reported herein were reproducible within ±10%. The potentials quoted are relative to an Ag|AgCl|3 M NaCl reference electrode.

the two redox couples in their respective phases and $\Delta^\circ_w\phi$, the Galvani potential difference at the liquid/liquid interface.[2] In the thin layer measurements, the potentials for the two ferrocenyl groups (obtained from Figure 1A) are the apparent formal potentials of **DFcB** in the organic phase, $E^{\circ\prime}_{NB} = E^{\circ\prime} + \Delta^\circ_w\phi$. The magnitude of $\Delta^\circ_w\phi$ accounts for the difference between these values and those determined by conventional solution electrochemistry.[19] When a redox couple with a formal potential of $E^{\circ\prime}_{H_2O}$ is placed in the aqueous phase (e.g., $[Fe(CN)_6]^{3-/4-}$), the overall driving force for the interfacial electron transfer will be $E^{\circ\prime}_{H_2O} - E^{\circ\prime}_{NB}$. In our studies, **DFcB** is the oxidant (in the **NB** phase) and $K_4Fe(CN)_6$ is the reductant (in the aqueous phase). The selection of $[Fe(CN)_6]^{3-/4-}$ as the redox couple in the aqueous phase was based on the following considerations: (1) as a standard outer-sphere redox couple, its formal potential is more negative than the formal potentials of both ferrocenyl groups of **DFcB**; (2) by taking advantage of the pH dependence of its formal potential, it is possible to alter the thermodynamic driving force for cross-phase electron transfer, which allows a complementary experiment. As shown in Figure 1B, the cyclic voltammogram of 1.0 mM $[Fe(CN)_6]^{4-}$ shifts significantly when one of the supporting electrolytes is changed from 0.1 M NaCl to 0.1 M HCl. The apparent formal potentials of the two ferrocenyl groups of **DFcB** in the **NB** phase and of $[Fe(CN)_6]^{4-}$ in two different supporting electrolytes are listed in Table 1.

When we added $[Fe(CN)_6]^{4-}$ to the aqueous phase and coated the working electrode with an **NB** thin layer containing **DFcB**, the current−potential responses changed from those shown in Figure 1A (without $[Fe(CN)_6]^{4-}$ in the aqueous phase) to those shown in Figure 2. In particular, the reversible peaks corresponding to the oxidation/reduction of **DFcB** in the **NB** layer disappeared; instead steady-state plateau currents were observed for varied concentrations of $[Fe(CN)_6]^{4-}$ (maintaining the concentration of **DFcB** in the **NB** layer constant at 22 μM). The two plateau currents in each of the current−potential curves shown in Figure 2 indicate that the electron transfer at the NB/H_2O interface occurs in two consecutive steps, corresponding to the oxidation of the first and the second ferrocenyl group (Scheme 1). These curves are similar to those reported by Shi and Anson[9e] for a thin layer of **NB** containing both decamethylferrocene (DMFc) and 1,1′,3,3′-tetrakis(2-methyl-2-hexyl)-ferrocene (MHFc) as co-reactants. In our study, the two electron transfer processes occur on the *same* molecule, thereby simplifying the comparison of the rate constants (see below). However, we note that the pairs of reactants exchanging electrons across the **NB**/water interface are still not identical at the two redox stages (Scheme 1).

The measured steady-state cathodic plateau current, i_{obs}, is jointly controlled by the rate of the cross-phase electron transfer reactions at the liquid/liquid interface and the diffusion of the reactant confined to the thin layer,[9b−d]

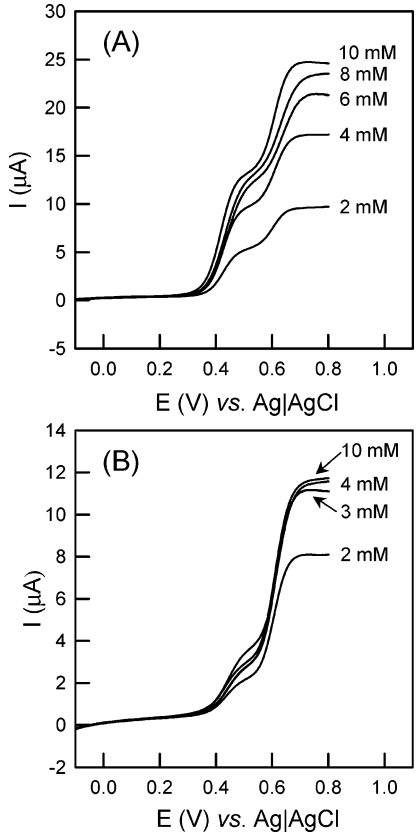

Figure 2. Current−potential curves recorded at a graphite electrode coated with 1.0 μL **NB** containing 2.20×10^{-2} mM **DFcB**, with $[Fe(CN)_6]^{4-}$ in the aqueous phase at different concentrations. The supporting electrolytes in aqueous phase were 0.1 M NaCl + 0.1 M $NaClO_4$ (A) and 0.1 M HCl + 0.1 M $NaClO_4$ (B); the supporting electrolyte in **NB** phase was 0.1 M TEAP. The scan rate was 5 mV/s.

$$\frac{1}{i_{obs}} = \frac{1}{i_d} + \frac{1}{i_{et}} \tag{1}$$

in which i_d and i_{et} are defined as

$$i_d = \frac{nFAC_{NB}D_{NB}}{\delta} \tag{2}$$

$$i_{et} = nFAk_{et}C_{NB}C_{H_2O} \tag{3}$$

where n is the number of electrons transferred, F is the Faraday constant, A is the area of the liquid/liquid interface (geometric area of the working electrode), C_{NB} is the concentration, D_{NB} is the diffusion coefficient of the reactant in **NB**, and δ is the

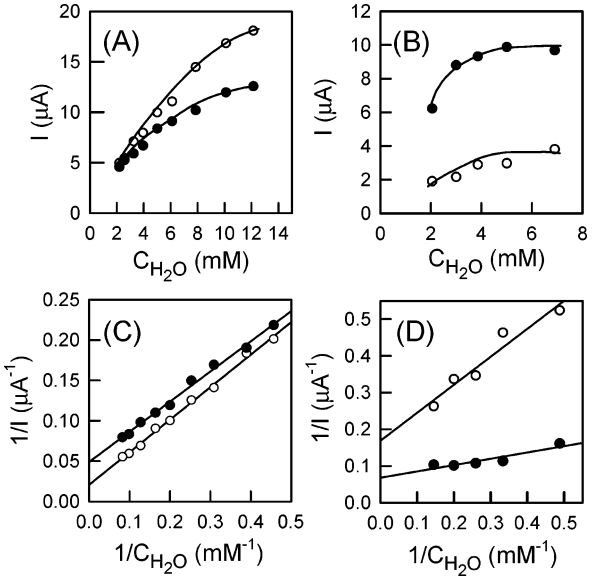

Figure 3. Cathodic plateau currents from Figure 2 as a function of the concentration of $[Fe(CN)_6]^{4-}$. The supporting electrolytes in the aqueous phase were 0.1 M NaCl + 0.1 M $NaClO_4$ (A) and 0.1 M HCl + 0.1 M $NaClO_4$ (B), respectively. Panels (C) and (D) plot the reciprocal plateau currents as a function of the reciprocal concentrations of $[Fe(CN)_6]^{4-}$, corresponding to the data shown in (A) and (B), respectively. In all cases, the plateau currents for step I (**DFcB**$^{+/0}$) are represented by open circles, and those for step II (**DFcB**$^{2+/+}$) by solid circles.

thickness of the **NB** layer coated on the electrode. The term of i_d stands for the current contribution limited by the diffusion of the reactant between the electrode surface and the liquid/liquid interface, and i_{et} indicates the current contribution caused by cross-phase electron transfer reaction. The k_{et} is the rate constant (cm s^{-1} M^{-1}) for the cross-phase electron transfer reaction.

Values of i_{obs}measured at different concentrations of $[Fe(CN)_6]^{4-}$ with different supporting electrolytes (from Figures 2A and 2B) are plotted in Figures 3A and 3B, respectively. It is clear that with increasing concentration of $[Fe(CN)_6]^{4-}$ the observed plateau currents for both electron transfer steps increase monotonically until they become concentration-independent, which is limited by the rate of diffusion of **DFcB** across the thin layer of **NB**. The selection of appropriate reactant concentrations in the two adjacent phases to minimize the effect of mass transfer on the measured currents has been discussed previously.[9d] We found that low concentrations of **DFcB** in **NB** (10−30 μM) and high concentrations of $[Fe(CN)_6]^{4-}$ (>1.0 mM) are required in order to obtain steady-state plateau currents for the present system. According to eqs 1 and 3, a plot of $1/i_{obs}$ versus $1/C_{H_2O}$ should be linear, and the bimolecular rate constant for the cross-phase electron transfer reactions, k_{et}, can be obtained from the slope of the fitting line. Shown in Figures 3C and 3D are two of these plots, corresponding to the data displayed in Figures 3A and 3B, respectively. Thus obtained rate constants for the two electron transfer steps in two different supporting electrolytes are listed in Table 1.

Unlike the reported dependences of cross-phase electron transfer rate constants (increase, decrease, or no change)[6c,7a,8,9c,e] on the Galvani potential difference $\Delta_w^o\phi$, reasonably consistent results have been obtained for redox couples with widely differing formal potentials in the adjoining phases.[6d,9c,e] As shown in Table 1, the observed correlation between the overall driving force and the bimolecular electron transfer rate constants agrees with the general trend reported previously. Under both neutral and acidic conditions, an increase of the thermodynamic driving force leads to a faster electron transfer at the interface, which is consistent with the results of previous investigations.[6d,9c,e] For example, Shi and Anson have observed a clear dependence of the bimolecular electron transfer rate constants on the overall driving force when using either $[DMFc]^+$ or $[ZnTPP]^+$ (ZnTPP = zinc tetraphenylporphyrin) in the organic phase and different reducing agents in the aqueous phase.[9c] For the $[ZnTPP]^+$ system, the overall driving force was varied from − 60 to +505 mV, and the reported rate constants increased from 0.8 to 1.8 cm s^{-1} M^{-1}. Ding et al.[6d] accumulated a comprehensive set of data to demonstrate the correlation by using the redox couples $[Ru(CN)_6]^{3-/4-}$, $[Mo(CN)_8]^{3-/4-}$, $[Fe(CN)_6]^{3-/4-}$, $[W(CN)_8]^{3-/4-}$, $[Fe(EDTA)]^{-/2-}$, $[Ru(NH_3)_6]^{3+/2+}$, $[Co(Sep)]^{3+/2+}$, and $V^{3+/2+}$ in the aqueous phase and 5,10,15,20-tetraphenyl-21*H*,23*H*-porphyrin zinc (ZnPor) in the organic phase; they observed that the electron transfer rate constant increases upon increased overall driving force up to 700 mV. Furthermore, the observed correlation between k_{et} and overall driving force in our system is also qualitatively in agreement with the conventional Butler−Volmer treatment, although more significant differences should be expected.[20,21] The much smaller sensitivity to driving force than predicted theoretically has been also reported by Shi and Anson at an **NB**/water interface using other reactant pairs, for which the sharpness of the interface was proposed as a contributing factor.[9c]

It should be noted that in the presence of 0.1 M HCl as part of the supporting electrolyte k_{et} increases more substantially with increasing driving force than with 0.1 M NaCl, although in both systems the changes are in the expected direction based on Butler−Volmer theory.[20] The origin of the variations in the behaviors observed for the two electrolytes remains to be fully understood, but possible differences in the self-exchange rate constants of ferrocenyl groups may be considered. This is due to the fact that in addition to the thermodynamic driving force of the reaction values of k_{et} also depend on the self-exchange rate constants of the two reactants.[21] Unfortunately, self-exchange rate constants for the ferrocenyl groups of **DFcB** in **NB** are not available at this stage.

The question of why in our system the kinetic data of electron transfer at liquid/liquid interfaces (Table 1) do not exhibit any simple reactivity pattern such as might be anticipated theoretically remains perplexing and deserves further experimental and theoretical study. Besides the different trends observed in the two electrolyte systems, for the **DFcB**$^{2+/+}$ redox couple the range of concentrations of $[Fe(CN)_6]^{4-}$ to obtain reproducible data for interfacial electron transfer is limited, particularly for the acidic supporting electrolyte system. We also did not obtain enough information (particular at higher driving force) for our redox couples to examine the applicability of Marcus' theory.[6d,22] Extensive studies to tackle these problems and the search for other novel molecules containing multiple redox centers (e.g., 1,1′-disubstituted oligomeric ferrocenes[23]) for cross-phase electron transfer studies are currently underway in our laboratory.

4. Conclusions

A new system has been proposed for the study of cross-phase electron transfer reactions at liquid/liquid interfaces, in which **DFcB**, an α,β-unsaturated ketone with two electrochemically nonequivalent ferrocenyl substituents, was chosen as redox couple in the organic phase. The thin-layer protocol has been shown not only to give a more distinct voltammetric response than conventional solution chemistry for bifunctional molecules but also to provide a simple way to evaluate the bimolecular rate constants for two-step cross-phase electron transfer pro-

cesses. Because these processes are associated with the two redox centers on the same reactant molecule at a single interface, the new system permits a reliable examination of the dependence of the cross-phase electron transfer kinetics on the overall thermodynamic driving forces.

Acknowledgment. The authors gratefully acknowledge the financial support from the Natural Sciences and Engineering Research Council of Canada (NSERC), from Simon Fraser University, and from Acadia University. We wish to thank Brian Hillier for his help with some preliminary experiments, and Dr. Eberhard Kiehlmann for reading the manuscript and informative discussions.

References and Notes

(1) (a) Girault, H. H. J.; Schiffrin, D. J. In *Charge and Field Effects in Biosystems*; Allen, M. J., Usherwood, P. N. R., Eds.; Abacus Press: Kent (UK), 1984; pp 171−178. (b) Matsuno, S.; Ohki, A.; Takagi, M.; Ueno, K. *Chem. Lett.* **1981**, 1543−1546. (c) Lillie, G. C.; Holmes, S. M.; Dryfe, R. A. W. *J. Phys. Chem. B* **2002**, *106*, 12101−12103.

(2) Girault, H. H. J.; Schiffrin, D. J. In *Electroanalytical Chemistry*; Bard, A. J., Ed.; Marcel Dekker: New York, 1989; Vol. 15, pp 1−141.

(3) Girault, H. H. J. In *Modern Aspects of Electrochemistry*; Bockris, J. O'M., Conway, B. E., White, R. E., Eds.; Plenum Press: New York, 1993; Vol. 25, pp 1−62.

(4) Samec, Z.; Mareček, V.; Koryta, J.; Khalil, M. W. *J. Electroanal. Chem.* **1977**, *83*, 393−397.

(5) For examples, see: (a) Girault, H. H. J.; Schiffrin, D. J. *J. Electroanal. Chem.* **1984**, *161*, 415−417. (b) Girault, H. H. J.; Schiffrin, D. J. *J. Electroanal. Chem.* **1988**, *244*, 15−26. (c) Geblewicz, G.; Schiffrin, D. J. *J. Electroanal. Chem.* **1988**, *244*, 27−37. (d) Cheng, Y.; Schiffrin, D. J. *J. Electroanal. Chem.* **1991**, *314*, 153−163. (e) Cheng, Y.; Schiffrin, D. J. *J. Chem. Soc., Faraday Trans.* **1994**, *90*, 2517−2523. (f) Ding, Z. F.; Fermín, D. J.; Brevet, P.-F.; Girault, H. H. *J. Electronanal. Chem.* **1998**, *458*, 139−148.

(6) (a) Wei, C.; Bard, A. J.; Mirkin, M. V. *J. Phys. Chem.* **1995**, *99*, 16033−16042. (b) Solomon, T.; Bard, A. J. *J. Phys. Chem.* **1995**, *99*, 17487−17489. (c) Tsionsky, M.; Bard, A. J.; Mirkin, M. V. *J. Phys. Chem.* **1996**, *100*, 17881−17888. (d) Ding, Z. F.; Quinn, B. M.; Bard, A. J. *J. Phys. Chem. B* **2001**, *105*, 6367−6374.

(7) (a) Liu, B.; Mirkin, M. V. *J. Am. Chem. Soc.* **1999**, *121*, 8352−8355. (b) Shao, Y.; Mirkin, M. V.; Rusling, J. F. *J. Phys. Chem. B* **1997**, *101*, 3202−3208.

(8) (a) Zhang, J.; Unwin, P. R. *J. Phys. Chem. B* **2000**, *104*, 2341−2347. (b) Zhang, J.; Barker, A. L.; Unwin, P. R. *J. Electroanal. Chem.* **2000**, *483*, 95−107.

(9) (a) Shi, C.; Anson, F. C. *Anal. Chem.* **1998**, *70*, 3114−3118. (b) Shi, C.; Anson, F. C. *J. Phys. Chem. B* **1998**, *102*, 9850−9854. (c) Shi, C.; Anson, F. C. *J. Phys. Chem. B* **1999**, *103*, 6283−6289. (d) Shi, C.; Anson, F. C. *J. Phys. Chem. B* **2001**, *105*, 1047−1049. (e) Shi, C.; Anson, F. C. *J. Phys. Chem. B* **2001**, *105*, 8963−8969.

(10) Shafer, H. O.; Derback, T. L.; Koval, C. A. *J. Phys. Chem. B* **2000**, *104*, 1025−1032.

(11) Park, H.; Higuchi, T.; Okazaki, S.; Oyama, M. *J. Electroanal. Chem.* **2002**, *518*, 27−32.

(12) Wang, R.; Okajima, T.; Kitamura, F.; Matsumoto, N.; Thiemann, T.; Mataka, S.; Ohsaka, T. *J. Phys. Chem. B* **2003**, *107*, 9452−9458.

(13) Erasmus, J. J. C.; Lamprecht, G. J.; Swarts, J. C.; Roodt, A.; Oskarsson, Å. *Acta Crystallogr.* **1996**, *C52*, 3000−3002.

(14) du Plessis, W. C.; Vosloo, T. G.; Swarts, J. C. *J. Chem. Soc., Dalton Trans.* **1998**, 2507−2514.

(15) du Plessis, W. C.; Erasmus, J. J. C.; Lamprecht, G. J.; Conradie, J.; Cameron, T. S.; Aquino, M. A. S.; Swarts, J. C. *Can. J. Chem.* **1999**, *77*, 378−386.

(16) Gupta, H. K.; Reginato, N.; Ogini, F. O.; Brydges, S.; McGlinchey, M. J. *Can. J. Chem.* **2002**, *80*, 1546−1554.

(17) Steiger, B.; Anson, F. C. *Inorg. Chem.* **2000**, *39*, 4579−4585.

(18) (a) Alvarez, J.; Kaifer, A. E. *Organometallics* **1999**, *18*, 5733−5734. (b) Flanagan, J. B.; Margel, S.; Bard, A. J.; Anson, F. C. *J. Am. Chem. Soc.* **1978**, *100*, 4278−4253, and references therein.

(19) An aqueous Ag|AgCl|3 M NaCl reference electrode is about 315 mV negative with respect to the nonaqueous $Ag|Ag^+$ (0.01 M $AgNO_3$ in acetonitrile) electrode; therefore, the apparent formal potentials of **DFcB**, obtained by thin layer voltammetry, would be 90 and 265 mV vs $Ag|Ag^+$, respectively. The estimated values of $\Delta^\circ_w\phi$ at this particular interface are −93 and −83 mV, which are identical to each other within the experimental uncertainty.

(20) Amemiya, S.; Ding, Z.; Zhou, J.; Bard, A. J. *J. Electroanal. Chem.* **2000**, *483*, 7−17.

(21) On the basis of eq 7, $k_{12} = \text{const} \exp(-\Delta G^{\ddagger}/RT)$, and eq 8, $\Delta G^{\ddagger} = \alpha F(\Delta E^\circ + \Delta^\circ_w\phi)$ in ref 20, the ratios of rate constants for the two redox steps are estimated to be 28.9 (in 0.1 M HCl) and 32.1 (in 0.1 M NaCl), assuming other constants in the equations are the same.

(22) Marcus, R. A. *J. Phys. Chem.* **1991**, *95*, 2010−2013.

(23) Marcus, R. A. *J. Chem. Phys.* **1965**, *43*, 679−701.

(24) (a) Roling, P. V.; Rausch, M. D. *J. Org. Chem.* **1972**, *37*, 729−732. (b) Brown, G. M.; Meyer, T. J.; Cowan, D. O.; LeVanda, C.; Kaufman, F.; Roling, P. V.; Rausch, M. D. *Inorg. Chem.* **1975**, *14*, 506−511.